Int. J. Electrochem. Sci., 15 **(2020)** 8471 – 8478, doi: 10.20964/2020.09.79

International Journal of
ELECTROCHEMICAL
SCIENCE
www.electrochemsci.org

Short Communication

Study on Preparation and Performance of PEO-PVDF Composite Binder for Lithium ion Batteries

Xinghua Liang[1,2,*], *Xi Wu*[1], *Yunting Wang*[1], *Xinqi Li*[1], *Qixin Gai*[1], *Jie Mao*[2]

[1] Guangxi Key Laboratory of Automobile Components and Vehicle Technology, Guangxi University of Science & Technology, Liuzhou 545006, China;
[2] National Engineering Laboratory for Modern Materials Surface Engineering Technology, Guangdong Institute of New Materials, Guangdong Academy of Science, Guangzhou 510650, China.
[*]E-mail: lxh304@aliyun.com (Xinghua Liang)

Received: 13 May 2020 / *Accepted:* 2 July 2020 / *Published:* 10 August 2020

PEO-PVDF composite binder was used to prepare lithium manganate positive pole piece and its phase and morphology were characterized by X-ray diffractometer (XRD) and scanning electron microscope (SEM). At the same time, CV, AC resistance and charge-discharge tests are used to perform electrochemical performance tests. The results appearanced that the specific discharge capacity of the battery declined from 113mAh / g to 88mAh / g after 150 cycles, and the Coulomb efficiency remains at about 99%. And the CV curve almost coincides with 100 times, which indicates excellent cycle performance.

Keywords: $LiMn_2O_4$; Lithium ion battery; Binder; PEO-PVDF; Cycle performance

1. INTRODUCTION

Lithium-ion batteries have the advantages of large specific capacity, good rate performance, high operating voltage, long cycle life, good safety performance, and ring mirror friendly. They are widely used in 3C electronic products, electric vehicles, and new energy storage[1-5]. Spinel lithium manganate ($LiMn_2O_4$) has a three-dimensional tunnel structure and good lithium removal performance. It has rich manganese resources, high discharge voltage, long cycle life, simple synthesis process, and good safety performance. This is considered to be the cathode material of choice for large-scale lithium-ion battery applications[6-9]. In the preparation of lithium batteries, the type and performance of the binder is critical to the performance of the battery. Binder is one of the important auxiliary materials for lithium ion batteries, which is mainly used in the preparation process of battery electrodes, and its dosage accounts for 5% to 10% of the positive and negative active materials[10-12]. The role of the binder is to ensure the uniformity and safety of the active material during the pulping process. Maintain the adhesion between the active material particles and the current collector, so that it can be wetted by the organic electrolyte. The binder has good processing properties and is not easy to burn. It is stable to electrolyte and has high electron ion conductivity. Low price and easy availability of raw materials are one of its rare advantages[13-15]. In terms of the effect of binders on the safety of lithium-ion batteries, studies have shown that when a slurry made of various binders is coated on copper foil without additives, the effect varies depending on the binder. If the adhesive is not good, the black film will fall off in a large area, which will seriously threaten the safety of the battery[16-17]. At present, polyvinylidene fluoride (PVDF) is widely used in the industrialization of oil-soluble binders. In recent years, the application as a binder in lithium batteries is the reason for its rapid growth in market consumption[18-19]. Factors that affect the performance of PVDF homopolymer binders for lithium batteries include the molecular weight and amount of PVDF added, the viscosity of the oil-soluble binder, the type of solvent, and the amount of coupling agent added[9].

Among them, the important factor affecting the performance is the molecular weight of PVDF[20]. If the molecular mass is too small, the amount of adhesive required will lead to poor bonding performance; If the molecular mass is too large, the solubility in the dispersion solvent is not good, the viscosity of the resulting slurry is too high and it is easy to form a gel, which is not conducive to mixing and coating. Therefore, in the case of ensuring normal dissolution and operating without violating regulations, high molecular weight PVDF should be used as much as possible. The average relative molecular mass of PVDF for lithium-ion batteries is preferably greater than 100,000[21], which can effectively reduce the amount of binder and improve the resistance of the electrode to the electrolyte corrosion, thereby enhancing the performance of the battery. At present, the research focus of the industrial application of oil-soluble binders is the modification of PVDF. The main modification methods are the copolymerization method and the blending method. The copolymerization method uses a small amount of second and third monomers to copolymerize with vinylidene fluoride (VDF) to improve the performance of PVDF[22]. For example, monomers such as chlorotrifluoroethylene or hexafluoropropylene are copolymerized with vinylidene fluoride. The blending method uses a mixture of two or more polymers as a binder for lithium-ion batteries. This method mixes polymers with good flexibility and viscoelasticity with PVDF to make up for their deficiencies[23]. No matter what method is used, it is mainly to reduce crystallinity, improve adhesion and appropriate molecular weight, and solve the problem of electrolyte swelling. The blending method is simpler than the copolymerization method, but selecting a second polymer with suitable properties matching the slurry system is the key to success. Ningbo Institute of Materials Xue Lixin et al. conducted research on polymer blending of ionic polymers PFSiLi and PVDF, and tested performance with lithium iron phosphate as the cathode material. The cathode shows better reversibility due to the ion composite binder, which improves the high-rate capacity and higher potential of the discharge platform at elevated temperature[24]; Zhejiang University Xie Jian et al. used PANi / PVDF composite binder with $CoSb_3$ as the active material. The results show that the $CoSb_3$ electrode with binary binder has a higher reversible capacity than the single PVDF binder in the initial cycle[25].

In this paper, lithium hydroxide ($LiOH{\cdot}H_2O$) and manganese acetate ($C_4H_6MnO_4 \cdot 4H_2O$) are used as precursors to prepare $LiMn_2O_4$ cathode material by high temperature solid-state method. Using PVDF binder and PVDF / PEO as composite binder to prepare two kinds of positive electrode sheet respectively. And through X-ray diffraction (XRD, D8Advance type, German Bruker company) spectrum, scanning electron microscope (SEM, ΣIGMA type, German Zeiss company), AC impedance (EIS, CH1660E type electrochemical workstation, Shanghai Chenhua Instrument Co., Ltd.) spectrum, Cyclic voltammetry (CV, CH1660E electrochemical workstation, Shanghai Chenhua Instrument Co., Ltd.) and battery tester (BTS4008W, Shenzhen New Will Electronics Co., Ltd.) analyzed the electrochemical performance of PVDF and PVDF / PEO binder impact and its causes.

2. EXPERIMENTAL

Synthesis of spinel lithium manganate by high temperature solid-state method. Use lithium hydroxide ($LiOH \cdot H_2O$) as the lithium source and manganese acetate ($C_4H_6MnO_4 \cdot 4H_2O$) as the manganese source. Weigh according to the stoichiometric ratio of $LiMn_2O_4$. Dissolve these in an appropriate amount of deionized water, and then put them into a ball mill ball milling. Finally, the ball-milled powder was placed in a muffle furnace and heated to 800 ° C at 5 ° C / min. Constant temperature for 24 hours, after the temperature was cooled to room temperature, the powder was taken out and ground to obtain spinel lithium manganate active material. Lithium manganate material, binder and conductive carbon black are mixed in an appropriate amount of NMP (N-methylpyrrolidone) at a mass ratio of 8: 1: 1, where the binder PVDF and PVDF / PEO blend polymer ratio is 8: 2. After stirring uniformly, the slurry is evenly coated on the aluminum foil current collector. The coated aluminum foil was dried in a vacuum oven at 80 ° C for 12 hours to obtain an electrode sheet. And use the electrode sheet as the working electrode, the lithium sheet as the counter electrode, and the cellgard 2400 polypropylene microporous membrane as the separator. Using a mixed solvent of $LiPF_6$ + EC/EMC/DMC (volume ratio 1: 1: 1) with a composition of 1mol / L as an electrolyte, assemble a CR2016 type button cell in a glove box filled with argon. The battery test system is used to test the charge and discharge performance of the button battery. The voltage range is set to 3-4.3V, and the charge and discharge test is performed at 0.2 C current.

3. RESULTS AND DISCUSSION

3.1 Phase composition and morphology analysis

Using X-ray diffraction method to conduct phase analysis on the electrode sheet made of PVDF, PEO and $LiMn_2O_4$, the XRD pattern of the scanning angle is set to $10^\circ \sim 90^\circ$. It can be seen from Figure 1 that the characteristic peaks of the spinel $LiMn_2O_4$ electrode sheet are completely consistent with the standard card PDF35-0782, and there are no PVDF and PEO peaks and other heterogeneous peaks. This phenomenon indicates that the addition of PEO as a binder has been completely dissolved in the NMP solvent. At this time, the low crystallinity of PEO did not affect the crystal structure of the $LiMn_2O_4$ electrode material, and thus did not affect the conductivity of the active material.

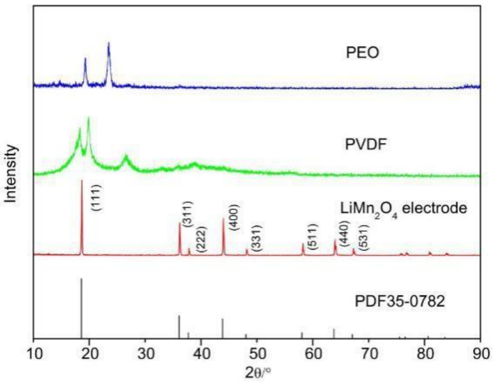

Figure 1. X-ray diffraction pattern of electrode sheets made of PVDF, PEO and $LiMn_2O_4$.

In order to study the effect of the composite binder PVDF / PEO on the spinel $LiMn_2O_4$ electrode, a field emission scanning electron microscope was used to analyze the $LiMn_2O_4$ electrode. It can be seen from Figure 2 (a) that the sample particles all have a regular octahedral geometry, and the particle surface is smooth and round. This indicates that the lithium manganate prepared by the solid phase sintering process has a good crystal structure and good conductivity. Figure 2 (b) shows that the $LiMn_2O_4$ electrode is relatively uniformly coated on the surface of the current collector, and micropores are observed. This is mainly due to the evaporation of the solvent during the drying of the pole piece. The addition of the polymer PEO connects the microstructures of the active materials to each other, thereby improving the ionic conductivity. Research by Sajid Hussain Siyal et al. also showed that the addition of PEO can improve the ionic conductivity and cycle stability of lithium-ion battery materials.[26]

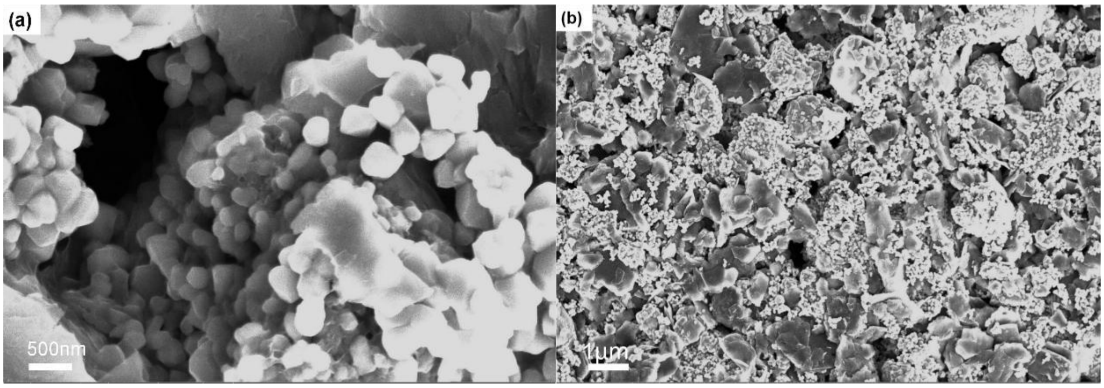

Figure 2. (a) SEM image of $LiMn_2O_4$ electrode prepared with PVDF binder, (b) SEM image of $LiMn_2O_4$ electrode prepared with composite binder PVDF / PEO.

At room temperature, use a battery tester to test the charge and discharge of the assembled button battery. The charge and discharge current density are set to 0.2C, and the charge and discharge cutoff voltages are 4.3V and 3V, respectively. Figure 3 (a) shows the first charge-discharge curve of $LiMn_2O_4$ battery using PVDF binder and PVDF/PEO mixed binder. It can be seen from the battery charge and discharge curve of the PVDF type binder that the first charge and discharge voltage platform is relatively stable, and the platform appears at 4.2V. The first charge-discharge specific capacity was 97mAh/g and

93.7mAh/g, and the charge-discharge efficiency was 96.5%. The higher charge-discharge efficiency may be due to the sufficient contact between the electrolyte and the active material, resulting in a more stable SEI film to ensure that the crystal structure of spinel $LiMn_2O_4$ is not easily collapsed when Li^+ is deintercalated, preventing irreversible cycling. Figure 3 (a) also shows that the $LiMn_2O_4$ battery with PVDF/PEO hybrid binder has better first-time charge-discharge performance, the discharge specific capacity is 112mAh/g, and the charge-discharge efficiency is 93%. During the discharge process, the voltage slowly dropped, and the discharge curve began to steepen after 3.9V, and then the termination voltage reached quickly, indicating that the battery has a high discharge voltage(＞4.2V) and a good discharge platform.It is consistent with the phenomenon that the electrochemical stability window of the PVDF/PEO binary binder was observed in literature[24,27] is above 5.0 V. This is higher than widely commercial application (4.2 V) for lithium ion batteries.

In order to verify the cycle performance of the battery, the assembled battery was tested for 150 charge and discharge cycles at a current of 0.2C at room temperature. Figure 3 (b) shows that the initial discharge specific capacity of the PVDF binder battery is 93mAh/g, which is only maintained at 66mAh/g after 150 cycles, and the Coulomb efficiency remains at about 96%. However, after 150 cycles of PVDF/PEO hybrid binder battery, the discharge specific capacity is reduced from 113mAh/g to 88mAh/g which implies that the reversible capacity of the binary binder PVDF/PEO is higher than that of the single type PVDF[25], and the Coulomb efficiency is maintained at about 99% that is consistent with the research conclusion of literature[28].This shows that compared with PVDF, the battery using PVDF / PEO hybrid binder has more excellent cycle performance. It can be seen that the cycle performance of the PVDF type battery is poor, which may be due to the decrease in the bonding strength of the binder as the number of battery cycles increases. The shedding of the active material of the positive electrode severely leads to a sharp increase in the internal resistance of the battery, resulting in a rapid decline in the cycle specific capacity of the battery.

Fig.3 (c) (d) shows the AC impedance spectrum of the battery of PVDF type and PVDF / PEO mixed binder respectively. The illustration is an equivalent circuit diagram for fitting the impedance and analyzing the diffusion performance of the battery impedance. Among them, the straight line with a slope of 45° in the low frequency region represents the diffusion impedance of Li^+, which is mainly used to evaluate the diffusion of Li^+ during battery charging and discharging. The semicircle from the high frequency to the low frequency region represents the electrochemical transmission impedance, mainly due to the impedance of the SEI film formed by the chemical reaction at the interface between the electrode and the electrolyte. The semi-circular arc of higher frequency is the electrode reaction impedance, and the intercept of the intersection point of the semi-circular arc at the high frequency end and the real axis is the ohmic impedance of the battery. Figure 3 (c) shows that the ohmic resistance of PVDF cells at 100 and 150 cycles is 962.7Ω and 985.23Ω, respectively. Figure (d) shows that the ohmic resistance of the PVDF / PEO hybrid binder battery at 100 and 150 cycles is 37.13Ω and 49.9Ω, respectively, and the impedance of the PVDF / PEO battery is significantly smaller than that of the PVDF battery. In Figure (d), there are two semi-circular arcs, which are mainly caused by the blending of PEO and PVDF polymer. The connection of the polymer chain provides more channels for Li^+ transportation, which improves the migration efficiency of Li^+.Consistent with the research conclusion of literature[29].

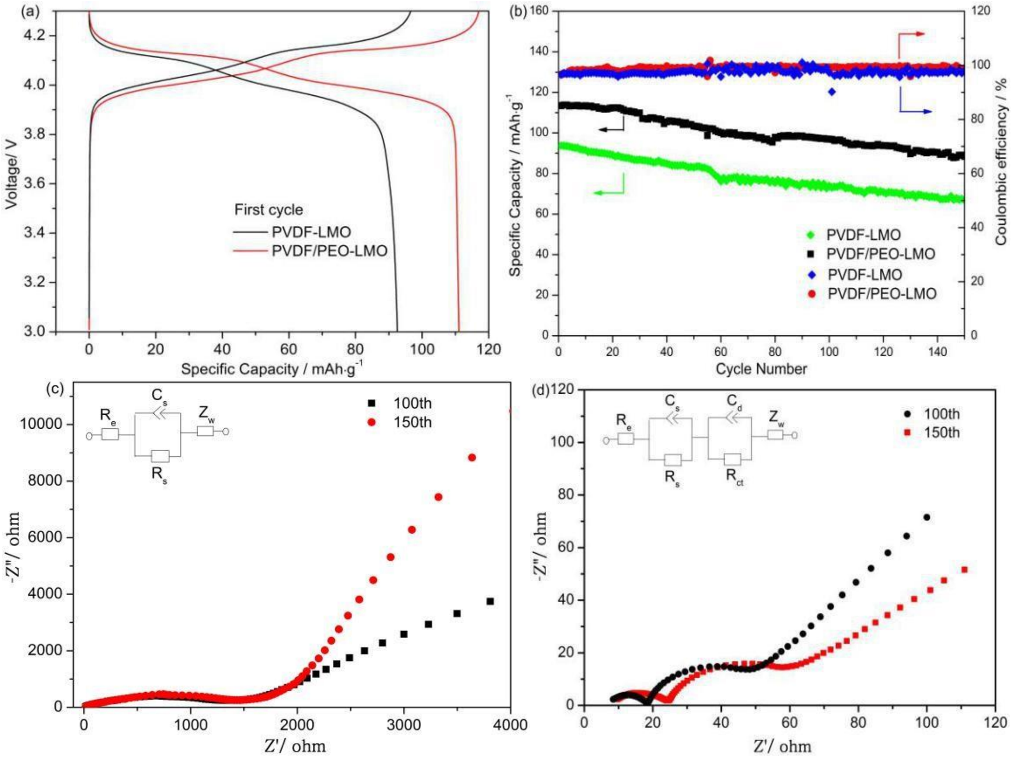

Figure 3. The (a) first charge discharge curve (b) 150 charge discharge cycle test curve and (c)(d) AC impedance spectrum of $LiMn_2O_4$ battery prepared by PVDF binder and PVDF / PEO mixed binder at 0.2C ratio.

Cyclic voltammetry is commonly used to study the redox process in electrode systems. The electrochemical window of the electrode, the position of redox and the corresponding peak value can be obtained by analyzing the CV curve to further evaluate the performance of the binder. Figure 4 (a) (b) shows the cyclic voltammetry curves of $LiMn_2O_4$ battery with PVDF and PVDF / PEO binder respectively. The scanning range of CV is 3.0 ~ 4.3V at 0.1mV / s. From Figure 4 (a) (b), we can see that two redox peaks appear in the battery during the cycle, which correspond to the change of Mn^{3+} valence state. When the battery is in 100 cycles, Figure 4 (a) shows that the battery using PVDF binder has oxidation peaks and reduction peaks around 3.9V / 4.1V and 4.1 / 4.24V, which indicates the process of Li^+ detaching and inserting from the cathode material during charging and discharging of the battery. From Figure 4 (b), the oxidation peak of $LiMn_2O_4$ battery with PVDF/PEO binder appears around 4.0V/4.18V, and the reduction peak appears around 4.1V/4.22V. In contrast, the voltage platform for battery discharge with PVDF / PEO binder has increased. After the battery has cycled 150 times, the CV curve at 150 times in Figure (a) has a larger drop than the peak value at 100 times, indicating that its cycle performance of the $LiMn_2O_4$ battery with PVDF binder was not ideal. The 150-time CV curve $LiMn_2O_4$ in Figure (b) almost coincides with 100 times, indicating that the PVDF / PEO binder $LiMn_2O_4$ battery has better cycle performance.

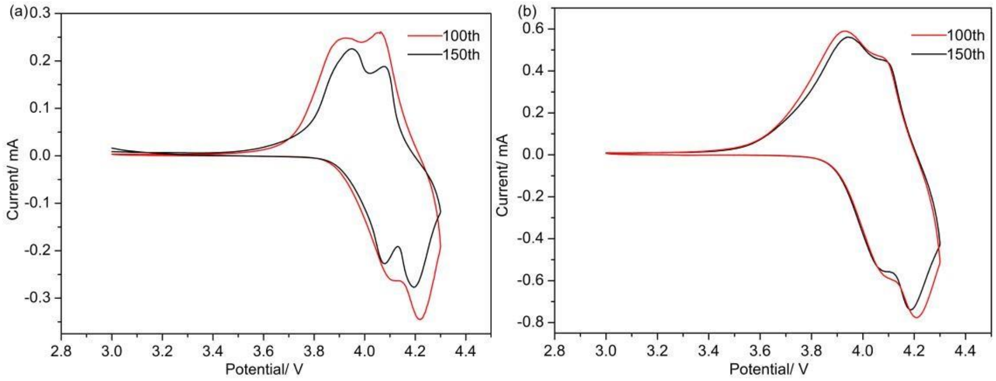

Figure 4. Cyclic voltammetry curves of $LiMn_2O_4$ cells prepared with (a) PVDF binder and (b) PVDF / PEO mixed binder at 0.1 mV / s.

4. CONCLUSIONS

Using PVDF / PEO as a composite binder to prepare a cathode using lithium manganate as the active material, and compared with the ordinary cathode. The polymer chain of PEO does not have a crystalline phase and does not affect the transmission of lithium ions. The presence of PEO not only plays a role in enhancing the transmission of lithium ions, but also plays a role in interface protection. The increase of the voltage platform and the improvement of the cycle performance both benefit from the two benefits of PEO. The ohmic resistance of the PVDF / PEO hybrid binder battery at 100 and 150 cycles is 37.13Ω and 49.9Ω, respectively. The impedance of the PVDF / PEO battery is significantly lower than that of the PVDF battery, thanks to the connection of the polymer chains produced by the blending of PEO and PVDF polymer. This connection provides more channels for Li^+ transportation, thereby improving Li^+ migration efficiency.

ACKNOWLEDGEMENTS
This work was supported by the Fund Project of the GDAS Special Project of Science and Technology Development, Guangdong Academy of Sciences Program (No. 2020GDASYL -20200104030); the Innovation Project of Guangxi University of Science and Technology Graduate Education (YCSW2020217); Guangxi Innovation Driven Development Project (No. AA18242036-2); and the Fund Project of the Key Lab of Guangdong for Modern Surface Engineering Technology (No. 2018KFKT01).

References

1. Jaesang Yoon, Mihee Jeong, In Tae Bae, Kyung-Wan Nam, Won-Sub Yoon, *Journal of Power Sources*, 368(2017)1-10.
2. M. Armand, J.-M. Tarascon, *Nature*, 451(2008)652–657.
3. Zhenguo Yang, Jianlu Zhang, Michael C. W. Kintner-Meyer, Xiaochuan Lu, Daiwon Choi, John P. Lemmon, Jun Liu, *Chemical Reviews*, 111(2011)3577-3613.
4. John B. Goodenough, Youngsik Kim, *Chemistry of materials*, 22(2010)587-603.
5. Zonghai Chen, Yan Qin, Khalil Amine, Y.-K. Sun, *Journal of Materials Chemistry*, 20(2010)7606-7612.

6. Vinodkumar Etacheri, Rotem Marom, Ran Elazari, Gregory Salitra, Doron Aurbach, *Energy & Environmental Science*, 4(2011)3243-3262.
7. Sevda Aktaş, Osman Murat Özkendir, Yasin Ramazan Eker, Şule Ateş, Ülfet Atav, Gültekin Çelik, Wantana Klysubun, *Journal of Alloys and Compounds*, 792(2019)279-285.
8. Qing Zhu, Shuai Zheng, Xuwu Lu, Yi Wan, Quanqi Chen, Jianwen Yang, Ling-zhi Zhang, Zhouguang Lu, *Journal of Alloys and Compounds*, 654(2016)384-391.
9. Artur Tron, Yeong Don Park, Junyoung Mun, *Journal of Power Sources*, 325(2016)360-364.
10. Yue Ma, Jun Ma, Guanglei Cui, *Energy Storage Materials*, 20(2019)146-175.
11. Woo-Jin Song, Se Hun Joo, Do Hyeong Kim, Chihyun Hwang, Gwan Yeong Jung, Sohyeon Bae, Yeonguk Son, Jaephil Cho, Hyun-Kon Song, Sang Kyu Kwak, Soojin Park, Seok Ju Kang, *Nano Energy*, 32(2017)255-262.
12. Yoon Hwa, Elton J. Cairns, *Electrochimica Acta*, 271(2018)103-109.
13. Wanjie Zhang, Mouad Dahbi, Shinichi Komaba, *Current Opinion in Chemical Engineering*, 13(2016)36-44.
14. Feng Wu, Weikang Li, Lai Chen, Yun Lu, Yuefeng Su, Wurigumula Bao, Jing Wang, Shi Chen, Liying Bao, *Journal of Power Sources*, 359(2017)226-233.
15. Marcus Müller, Lukas Pfaffmann, Stefan Jaiser, Michael Baunach, Vanessa Trouillet, Frieder Scheiba, Philip Scharfer, Wilhelm Schabel, Werner Bauer, *Journal of Power Sources*, 340(2017)1-5.
16. Rui Xu, Jun Lu, Khalil Amine, *Advanced Energy Materials*, 5(2015)1-22.
17. Shu-Lei Chou, Yuede Pan, Jia-Zhao Wang, Hua-Kun Liu, Shi-Xue Dou, *Physical Chemistry Chemical Physics*, 16(2014)20347-20359.
18. T.A. Otitoju, A.L. Ahmad, B.S. Ooi, *Journal of Water Process Engineering*, 14(2016)41-59.
19. Wanjie Zhang, Mouad Dahbi, Shinichi Komaba, *Current Opinion in Chemical Engineering*, 13(2016)36-44.
20. George Zapsas, Yogesh Patil, Yves Gnanou, Bruno Ameduri, Nikos Hadjichristidis, *Progress in Polymer Science*, 104(2020)101231.
21. Seoungwoo Byun, Jaecheol Choi, Youngjoon Roh, Danoh Song, Myung-Hyun Ryou, Yong Min Lee, Electrochimica Acta, 332(2020)135471.
22. E.P Roth, D.H Doughty, J. Franklin, *Journal of Power Sources*, 134(2004)222-234.
23. Samira Maazi, Amir H. Navarchian, Mohsen Khosravi, Pu Chen, *Solid State Ionics*, 320(2018)84-91.
24. Qianru Shi, Lixin Xue, Zengbin Wei, Fu Liu, Xudong Du, Darryl D.DesMarteau, *Journal of Materials Chemistry A*, 1(2013)15016-15021.
25. Xie Jian, Z Xinbing, Cao Gaoshao, *Journal of Materials Science & Technology*, 1(2007)144-146.
26. Sajid Hussain Siyal, Mengjie Li, Hao Li, Jin-Le Lan, Yunhua Yu, Xiaoping Yang, *Applied Surface Science*, 494(2019)1119-1126.
27. Fangli Deng, Xiaoen Wang, Dan He, Ji Hu, Chunli Gong, Yun Sheng Ye, Xiaolin Xie, Zhigang Xue, *Journal of Membrane Science*, 491(2015)82-89.
28. Xiuli Wang, Xiaojing Hao, Zhang Hengjing, Xinhui Xia, Jiangping Tu, *Electrochimica Acta*, 329(2020)135108.
29. Qizhen Xiao, Xingzhu Wang, Wen Li, Zhaohui Li , Tianjing Zhang, Hailiang Zhang, *Journal of Membrane Science*, 334(2009)117-122.